Fermi Surface and van Hove Singularities in the Itinerant Metamagnet $Sr_3Ru_2O_7$

A. Tamai,[1,*] M. P. Allan,[1] J. F. Mercure,[1] W. Meevasana,[2] R. Dunkel,[2] D. H. Lu,[2] R. S. Perry,[3] A. P. Mackenzie,[1] D. J. Singh,[4] Z.-X. Shen,[2] and F. Baumberger[1]

[1]*Scottish Universities Physics Alliance, School of Physics and Astronomy, University of St. Andrews, North Haugh, St. Andrews, Fife KY16 9SS, United Kingdom*

[2]*Departments of Applied Physics and Physics, and Stanford Synchrotron Radiation Laboratory (SSRL), Stanford University, Stanford, California 94305, USA*

[3]*Scottish Universities Physics Alliance, School of Physics and Centre for Science at Extreme Conditions, The University of Edinburgh, Mayfield Road, Edinburgh, EH9 3JZ, United Kingdom*

[4]*Materials Science and Technology Division, Oak Ridge National Laboratory, Oak Ridge, Tennessee 37831-6114, USA*

(Received 6 March 2008; published 11 July 2008)

The low-energy electronic structure of the itinerant metamagnet $Sr_3Ru_2O_7$ is investigated by angle-resolved photoemission and density-functional calculations. We find well-defined quasiparticle bands with resolution-limited linewidths and Fermi velocities up to an order of magnitude lower than in single layer Sr_2RuO_4. The complete topography, the cyclotron masses, and the orbital character of the Fermi surface are determined, in agreement with bulk sensitive de Haas–van Alphen measurements. An analysis of the d_{xy} band dispersion reveals a complex density of states with van Hove singularities near the Fermi level, a situation which is favorable for magnetic instabilities.

DOI: 10.1103/PhysRevLett.101.026407 PACS numbers: 71.18.+y, 71.20.−b, 75.30.Kz, 79.60.−i

Quantum criticality in correlated electron systems continues to attract widespread attention. One reason is that systems near a quantum critical point are highly susceptible to novel ordered phases, the observation and characterization of which promises new insight in the behavior of strongly interacting systems [1,2]. Possibly even more exciting is the prospect that fluctuations associated with a quantum critical point could dominate the phase diagram of topical materials, including the cuprate superconductors up to high temperatures [3]. Evidence for quantum critical points, reached by tuning pressure, chemical composition, or magnetic field, has been observed in a variety of materials comprising simple metals [4], heavy fermion intermetallics [5], or transition metal oxides such as $Sr_3Ru_2O_7$, the subject of this study [2,6].

Criticality in $Sr_3Ru_2O_7$ is associated with a metamagnetic transition (superlinear rise in magnetization) of the itinerant electron system in applied field. In the ground state, $Sr_3Ru_2O_7$ is a paramagnetic Fermi liquid with strongly enhanced quasiparticle masses. Its electronic specific heat value of $\gamma = 110\ \mathrm{mJ/mol\,Ru\,K^2}$ is among the highest in any oxide, and the large magnetic susceptibility indicates a substantial Stoner enhancement [7]. The Fermi liquid region of the phase diagram extends up to 10–15 K in zero field and is continuously suppressed towards zero temperature upon approaching the critical field of $B \approx 8$ T (for $B \parallel c$) [6]. In the vicinity of the putative quantum critical end point, non-Fermi-liquid behavior has been observed in various macroscopic quantities including specific heat, resistivity, and thermal expansion and has been described on the basis of phenomenological models [6,8–10].

On the other hand, little is known about the microscopic origin of the metamagnetism. Theoretical work suggests that the phase diagram of $Sr_3Ru_2O_7$ may be understood from peculiarities in the band structure causing either a local minimum in the density of states (DOS) at the Fermi level $\rho(E_F)$ or a sharp increase in DOS over the minute energy scale of the Zeeman splitting ($\approx$1 meV for $B =$ 10 T) [11–13]. Density-functional calculations for $Sr_3Ru_2O_7$ show a number of sharp features in the DOS [14] and have been invoked to support a band-structure-based model of metamagnetism, although their precision hardly reaches the 1 meV scale. Thus, experimental information on the evolution of the DOS near the Fermi level is key to advancing the field. A recent spectroscopic STM study detected peaks in the tunneling conductivity around ± 4 meV, which might be interpreted as a set of van Hove singularities in the DOS [15]. Published photoemission studies, on the other hand, did not report unusual features on the relevant energy scale [16,17].

In this Letter, we present a comprehensive high-resolution k-space mapping of the quasiparticle band structure in $Sr_3Ru_2O_7$ by means of angle-resolved photoemission spectroscopy (ARPES). We characterize the d_{xy} DOS in the vicinity of the chemical potential: We identify two peaks in $\rho(\epsilon)$ at -4 and -1 meV and discuss their relevance for metamagnetism.

Photoemission experiments were performed with a monochromatized He-discharge lamp and a Scienta SES2002 analyzer using an energy and angular resolution of 4.5 meV/0.3° full width at half maximum. Additional data at various excitation energies were taken at beam line V-4 of SSRL using a Scienta R4000 analyzer with a combined resolution set to 8.0 meV/0.3°. All data shown in this Letter were measured with 21.2 eV photons at $T =$ 9 K and a pressure $< 5 \times 10^{-11}$ mbar. High purity single crystals of $Sr_3Ru_2O_7$ were grown in an image furnace [18]. The detection of sizable quantum oscillations in all

samples used for this study indicates residual in-plane resistivities $<0.5\ \mu\Omega\,\mathrm{cm}$. Band-structure calculations in the local density approximation (LDA) were performed using the general potential linearized augmented plane wave method [19] with well-converged basis sets and zone samplings. Including spin-orbit interaction was found to improve the agreement with experiment. The Fermi surface is based on first-principles calculations at 850 k points in the irreducible 1/8 wedge of the zone using the experimental crystal structure [20].

We start by discussing the Fermi surface of $Sr_3Ru_2O_7$. A single bilayer of RuO_6 octahedra contains 4 Ru^{4+} ions, each contributing 4 conduction electrons distributed over the 3 nearly degenerate t_{2g} levels. Hence, in a first approximation one expects up to 12 bands crossing the Fermi level. Indeed, an earlier electronic structure calculation showed a highly fragmented Fermi surface suggesting that its experimental determination could be beyond current capabilities [14]. On the other hand, de Haas–van Alphen (dHvA) experiments found only 5 distinct frequencies corresponding to Fermi surface pockets in the range of 1.1%–32% of the Brillouin zone (BZ) area [21,22].

Figure 1(a) shows the experimental ARPES Fermi surface (FS) map. The data have been integrated over ± 2 meV, resulting in an effective energy resolution (convolution of integration window and spectrometer resolution) of 5.5 meV [23]. The identification of three Fermi surface pockets centered at Γ is straightforward from an analysis of individual cuts. The innermost sheet, labeled δ, is nearly circular. Remarkably, its orbital character, as inferred from LDA calculations, is Ru $d_{x^2-y^2}$; i.e., it belongs to the e_g manifold, which is unoccupied in Sr_2RuO_4 and $Ca_3Ru_2O_7$ [24–26]. The larger square- and cross-shaped holelike Fermi surfaces with pronounced uniaxial anisotropy derive from the out-of-plane $d_{xz,yz}$ orbitals. Around the M points, a small lens (β) and a larger lens with backfolded vertices (γ_1) can be identified. The shape of these pockets indicates mixing of $d_{xz,yz}$ and d_{xy} orbital character on the γ_1 sheet and a dominant $d_{xz,yz}$ character for the β sheet. The smaller lens is well resolved in the Fermi surface map, while the precise contours of the larger γ_1 pocket are more difficult to extract. However, its Fermi crossings along the $\Gamma M\Gamma$ line can clearly be identified from the cut shown in Fig. 2. A pronounced shoulder on the left-hand side of the γ_1 peak indicates a small bilayer splitting of this pocket, consistent with the density-functional theory (DFT) calculations. The intensity maxima in Fig. 1(a) connecting the edges of the γ_1 pockets between adjacent M points stem from a putative small hole pocket (γ_2) that is barely touching the Fermi surface. We find the top of this band located at -1 ± 1 meV (compare Fig. 3). Hence, based on the ARPES data alone, we cannot decide unambiguously whether it contributes to the Fermi surface. A slight k_z dispersion or a minute structural difference between the surface and bulk might be sufficient to lift the γ_2 pocket up to the Fermi level for a considerable fraction of the 3D bulk BZ.

The volumes A of all Fermi surface pockets are summarized in Table I and compared with recent de Haas–van Alphen data [27]. Cyclotron masses $m^* = \frac{\hbar^2}{2\pi} \times (\partial A/\partial \epsilon)_{k_F}$ have been calculated for individual pockets using Fermi velocities determined along several k-space cuts. The agreement is good for the volumes and well within the experimental error for the masses. This strongly suggests that the electronic structure seen by ARPES is nearly converged to that of the bulk. Nevertheless, we cannot exclude minute energy differences between the surface and bulk, which could lift the γ_2 pocket up to the Fermi level. To investigate this issue, we calculate the specific heat and the Luttinger volume based on the ARPES data [28]. We tentatively assign multiplicities by assuming a small bilayer splitting of the δ and γ_1 pockets, which is unresolved experimentally, and a twofold degeneracy of γ_2 as found in the DFT calculations. With these assumptions, we find $\Sigma m^* = 171(36) m_e$ [$91(16) m_e$] corresponding to $\gamma = 127(27)$ mJ/mol Ru K^2

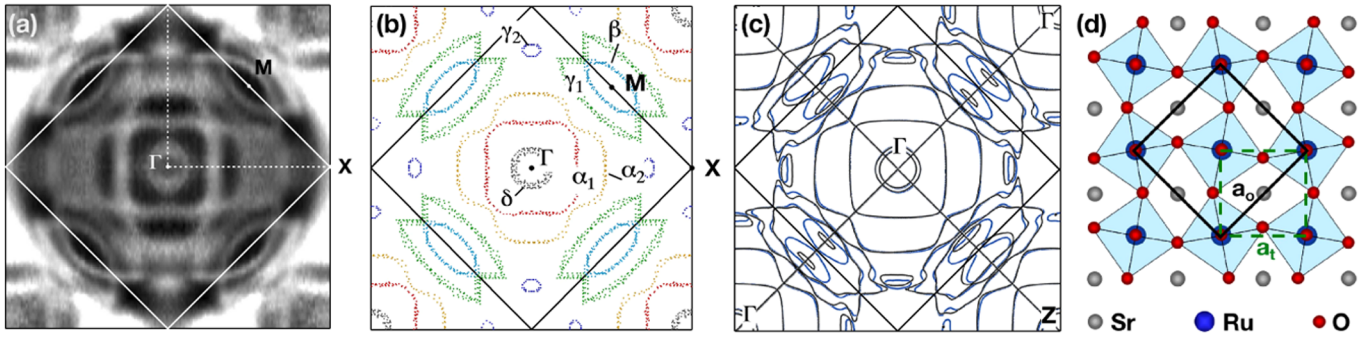

FIG. 1 (color online). Fermi surface of $Sr_3Ru_2O_7$. (a) shows the experimental data taken in the first quadrant of the larger tetragonal BZ and symmetrized with respect to the Ru-Ru nearest neighbor direction. X denotes the surface projection of R and M that of a midpoint between two Γ points (Z or S). (b) Fermi surface contours extracted from the data shown in (a). (c) LDA calculation for the basal plane ($k_z = 0$, black) and midplane ($k_z = 1/4$, blue). (d) Schematic structure of a single RuO_2 plane illustrating the unit-cell doubling due to a 6.8° rotation of the RuO_6 octahedra [20]. a_t denotes the Ru-Ru nearest neighbor distance and a_o the in-plane lattice constant of the orthorhombic unit cell, respectively.

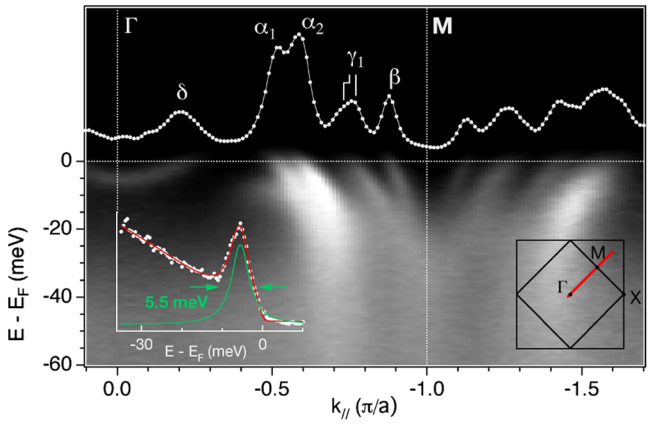

FIG. 2 (color online). Band dispersion along $\Gamma M\Gamma$. The Fermi surface crossings are labeled above the momentum distribution curve extracted at E_F. The inset shows a spectrum at the Γ point. A peak width of 5.5 meV in the raw data indicates an excellent surface quality.

[67(12) mJ/mol Ru K^2] with [without] counting the γ_2 pocket. Hence, comparing with the direct measurement of 110 mJ/mol Ru K^2 [7] suggests that γ_2 does contribute to the bulk specific heat and must be included in the zero field Fermi surface. The above scenario is consistent with the Luttinger volume of a compensated metal with an even number of valence electrons. Assuming an upper bound of $1 \pm 1\%$ BZ for A_{γ_2} we find $2(-A_{\alpha_1} - A_{\alpha_2} + 2A_\beta + 4A_{\gamma_1} - 8A_{\gamma_2} + 2A_\delta) = -0.24(25)$ electrons/RuO_2 bilayer or $-0.06(6) + 2n$ electrons/Ru ($n \in \mathbf{N}$).

Note that the high-energy resolution and ultraclean samples employed in this study were instrumental to resolve the Fermi surface of $Sr_3Ru_2O_7$. Some carrier pockets show occupied band widths of only ≈ 5 meV and Fermi velocities as low as 1.2×10^4 m/s (0.08 eV Å), approximately an order of magnitude lower than in single layer Sr_2RuO_4. An energy resolution >10 meV or impurity scattering contributions of this order to the linewidth, as are commonly observed by ARPES on transition metal oxides, would render it impossible to resolve such narrow bands. In order to illustrate the present data quality, we show an energy distribution curve (EDC) in the inset in Fig. 2 demonstrating a raw quasiparticle linewidth (including a 4.5 meV contribution from the experimental resolution) of 5.5 meV. This is narrower than state-of-the-art ARPES data from noble metal surface states [29] and is rarely seen in complex oxides.

The determination of the Fermi surface in agreement with bulk measurements allows for a more in-depth discussion of the electronic structure of $Sr_3Ru_2O_7$ based on the ARPES data. To this end, we will evaluate the density of states near the Fermi level of the γ_1, γ_2 sheets with significant d_{xy} contributions. Figure 3(a) shows the band topography along the $\Gamma X\Gamma$ line. A very narrow dispersion with local minima and maxima separated by less than 3 meV is observed over an extended k-space range, indicating a very high DOS just below the Fermi surface. The top of the band corresponding to the putative γ_2 Fermi surface pocket is observed at -1 ± 1 meV with a second local maximum at the X point near -3 meV. In order to obtain quantitative information on the d_{xy} density of states, we have analyzed the lowest lying excitation at each k point in a high-resolution k-space map covering the relevant area. The resulting contour plot is shown in Fig. 3(c). Saddle points in the dispersion corresponding to van Hove singularities in the density of states are found symmetrically around the X point, at an energy of -4 meV. Indeed, a histogram of the $\epsilon(k)$ values shows a sharp peak at this energy. A second peak related to the top of the band is observed around -1 meV, coincident with the natural energy scale of metamagnetism. We emphasize that $\rho(\epsilon)$ obtained in this way is not influenced by matrix-element effects since it is based on counting eigenstates rather than on measuring intensities [30]. Neither is the precision of $\rho(\epsilon)$ limited by the experimental energy resolution of 4.5 meV. It is given by the uncertainty in fitted peak positions, which is dominated by small variations (<2 meV) in measured peak positions between different experimental runs.

The sharp peaks in the density of states on the energy scale of the Zeeman splitting shown in Fig. 3(d) are qualitatively similar to the situation considered by Binz and Sigrist in their microscopic model of the metamagnetic transition [11]. This motivates a brief and speculative discussion of the effects of an applied field on the electronic structure of $Sr_3Ru_2O_7$. The pocket most likely to be strongly affected is γ_2, which could become completely spin polarized in a field of order 10 T. Since it is repeated 8 times in the BZ each spin-polarized pocket would need only to be modest in area to account for the moment change of $\approx 0.25\mu_B$ at the metamagnetic transition of $Sr_3Ru_2O_7$. The holelike character of γ_2 further means that, if it dominated the spin polarization in a rigid-band picture,

TABLE I. Fermi surface volumes and cyclotron masses of $Sr_3Ru_2O_7$ obtained from ARPES and dHvA. The polarity and dominant orbital character of the pockets is indicated in brackets. Errors are estimated from the statistical accuracy of the analysis and the reproducibility of the experiments. The mass of γ_2 is estimated from parabolic fits to the dispersion.

	$\alpha_1(h^+, xz, yz)$	$\alpha_2(h^+, xz, yz)$	$\beta(e^-, xz, yz)$	$\gamma_1(e^-, xy/xz, yz)$	$\gamma_2(h^+, xy)$	$\delta(e^-, x^2 - y^2)$
ARPES FS-volume A (% BZ)	14.1 ± 2	31.5 ± 3	2.6 ± 1	8.0 ± 2	<1	2.1 ± 1
ARPES cyclotron mass m^* (m_e)	8.6 ± 3	18 ± 8	4.3 ± 2	9.6 ± 3	10 ± 4	8.6 ± 3
dHvA FS-volume A (% BZ)	13.0 ± 1.0	30.1 ± 1.1	1.1 ± 0.2	6.6 ± 0.9	⋯	3.1 ± 0.3
dHvA cyclotron mass m^* (m_e)	6.9 ± 0.1	10.1 ± 0.1	5.6 ± 0.3	7.7 ± 0.3	⋯	8.4 ± 0.7

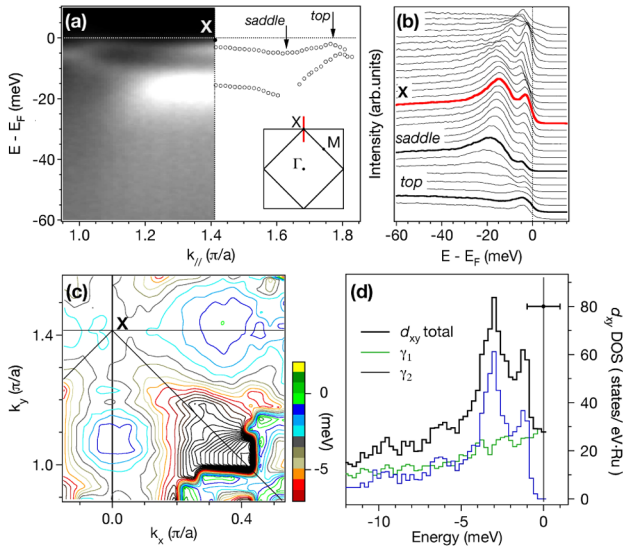

FIG. 3 (color online). Band dispersion around the van Hove singularities of the d_{xy} band. (a) Photoemission intensity in the vicinity of the X point along the direction marked in the inset. Peak positions have been determined by a fit to the energy distribution curves after normalization with the Fermi function. (b) Raw EDCs extracted from the data shown in (a). The high intensity above the Fermi level for $k_{\|}$ near the top of the band hints at the presence of unoccupied states within a few meV of the Fermi level. (c) Contour plot showing the energy position of the lowest lying quasiparticle excitation as a function of (k_x, k_y). (d) Histogram of near-E_F k states obtained from the band contours shown in (c). Absolute values are calculated assuming a twofold degeneracy (or an unresolved bilayer splitting) of $\gamma_{1,2}$. The total density of states $\rho(E_F)$ calculated from the measured specific heat is 47 states/eV Ru. The horizontal error bar in (d) indicates a ± 1 meV uncertainty in absolute $\epsilon(k)$ values estimated from the variation between different measurements.

one would expect an accompanying decrease in the areas of the holelike sheets α_1 and α_2 or an increase in the areas of the electron like β and γ_1 sheets. Intriguingly, a pronounced decrease of α_1 and α_2 was reported in Ref. [21], pointing towards an interorbital charge transfer from the d_{xy} to the $d_{xz,yz}$ sheet at the metamagnetic transition of $Sr_3Ru_2O_7$. Further investigation of these issues by detailed de Haas–van Alphen studies and scanning tunneling spectroscopy in high field are desirable.

In conclusion, we have presented high-resolution ARPES data from $Sr_3Ru_2O_7$. In combination with new LDA calculations incorporating spin-orbit coupling, the results allow an unambiguous identification of most Fermi surface pockets and of their dominant orbital character. Moreover, our data provide clear evidence for sharp spikes in the quasiparticle density of states on the natural energy scale of metamagnetism.

This work has been supported by the Scottish Funding Council and the U.K. EPSRC. SSRL is operated by the DOE's office of Basic Energy Science. Work at ORNL was supported by DOE BES, Division of Materials Science and Engineering.

*anna.tamai@st-andrews.ac.uk

[1] S. Sachdev, Science **288**, 475 (2000).
[2] R. Borzi *et al.*, Science **315**, 214 (2007).
[3] C. M. Varma, Phys. Rev. B **55**, 14 554 (1997).
[4] A. Yeh, Y.-A. Soh, J. Brooke, G. Aeppli, T. F. Rosenbaum, and S. M. Hayden, Nature (London) **419**, 459 (2002).
[5] G. R. Stewart, Rev. Mod. Phys. **73**, 797 (2001).
[6] S. A. Grigera *et al.*, Science **294**, 329 (2001).
[7] S.-I. Ikeda, Y. Maeno, S. Nakatsuji, M. Kosaka, and Y. Uwatoko, Phys. Rev. B **62**, R6089 (2000).
[8] A. J. Millis, A. J. Schofield, G. G. Lonzarich, and S. A. Grigera, Phys. Rev. Lett. **88**, 217204 (2002).
[9] P. Gegenwart, F. Weickert, M. Garst, R. S. Perry, and Y. Maeno, Phys. Rev. Lett. **96**, 136402 (2006).
[10] R. S. Perry *et al.*, Phys. Rev. Lett. **86**, 2661 (2001).
[11] B. Binz and M. Sigrist, Europhys. Lett. **65**, 816 (2004).
[12] C. Honerkamp, Phys. Rev. B **72**, 115103 (2005).
[13] E. P. Wohlfarth and P. Rhodes, Philos. Mag. **7**, 1817 (1962).
[14] D. J. Singh and I. I. Mazin, Phys. Rev. B **63**, 165101 (2001).
[15] K. Iwaya *et al.*, Phys. Rev. Lett. **99**, 057208 (2007).
[16] A. V. Puchkov, Z. X. Shen, and G. Cao, Phys. Rev. B **58**, 6671 (1998).
[17] Y. Aiura *et al.*, Phys. Rev. Lett. **93**, 117005 (2004).
[18] R. S. Perry and Y. Maeno, J. Cryst. Growth **271**, 134 (2004).
[19] D. J. Singh and L. Nordstrom, *Plane Waves, Pseudopotentials and the LAPW Method* (Springer, Berlin, 2006), 2nd ed.
[20] H. Shaked, J. D. Jorgensen, O. Chmaissem, S. Ikeda, and Y. Maeno, J. Solid State Chem. **154**, 361 (2000).
[21] R. A. Borzi *et al.*, Phys. Rev. Lett. **92**, 216403 (2004).
[22] R. S. Perry *et al.*, Phys. Rev. Lett. **92**, 166602 (2004).
[23] The orthorhombic crystal structure of $Sr_3Ru_2O_7$ (space group *Bbcb* [20]) lacks the fourfold symmetry of Sr_2RuO_4. However, our LDA calculations show that the Ru-Ru nearest- and next-nearest neighbor directions may be treated as approximate symmetry planes in the band structure. In our experiments, we could not resolve a breaking of these symmetries. Hence, we present the data in Fig. 1(a) symmetrized along ΓX.
[24] A. Damascelli *et al.*, Phys. Rev. Lett. **85**, 5194 (2000).
[25] F. Baumberger *et al.*, Phys. Rev. Lett. **96**, 107601 (2006).
[26] A. P. Mackenzie *et al.*, Phys. Rev. Lett. **76**, 3786 (1996).
[27] The values shown here are from very recent measurements [J. F. Mercure *et al.* (unpublished)] with higher precision than those reported in Ref. [21].
[28] F. Baumberger *et al.*, Phys. Rev. Lett. **96**, 246402 (2006).
[29] F. Reinert, G. Nicolay, S. Schmidt, D. Ehm, and S. Hüfner, Phys. Rev. B **63**, 115415 (2001).
[30] Here we assume that matrix elements of all bands in the relevant energy scale are finite and no bands eluded detection.